Impact Angle and Field-of-View Constrained Guidance Law Against Non-Maneuvering Moving Tank Using Nonlinear Virtual Relative Model and Optimal Error Dynamics

Hai Tran Van *, Dien Nguyen Ngoc, Dung Pham Trung, and Tung Thanh Nguyen

Institute of Missile and Control Engineering, Le Quy Don Technical University, Ha Noi, Viet Nam
Email: tranvanhai@lqdtu.edu.vn (H.T.V.); Bauman252@lqdtu.edu.vn (D.N.N.);
Phamtrungdung@lqdtu.edu.vn (D.P.T.); Nguyenthanhtung@lqdtu.edu.vn (T.T.N.)
*Corresponding author

***Abstract*—This paper presents an advanced guidance law design for Anti-Tank Guided Missiles (ATGM) attacking non-maneuvering moving tanks. The proposed method integrates constraints on impact angle and addresses the Field of View (FOV) limitation of the missile seeker during the final guidance phase. Using a nonlinear virtual relative model, this method treats moving targets as stationary. The paper also introduces an optimal form of error dynamics that allows the impact angle error to converge to zero within a finite time. A specially designed weighting function optimizes the distribution of command acceleration, effectively minimizing initial guidance commands and ensuring that command magnitudes gradually reduce to zero as the missile approaches the target. A saturation function is included to effectively manage the maximum FOV angle constraint, ensuring continuous target lock capabilities of the seeker throughout the missile's flight. Numerical simulations have demonstrated the robustness and increased accuracy of the proposed guidance law in achieving precise impact angles while maintaining operational constraints. The results highlight the potential of the proposed model in significantly enhancing the tactical effectiveness of ATGM systems in actual combat scenarios.**

***Keywords*—guidance law, impact angle, field-of-view, nonlinear virtual relative model, optimal error dynamics**

I. Introduction

Terminal guidance refers to the guidance applied to a missile between the midcourse phase and its arrival near the target. The terminal guidance law is a rule or control algorithm used to steer a missile toward its target in the final phase of flight. This is the most critical phase, immediately before the weapon impacts, requiring high precision to ensure the target is effectively destroyed [1].

Specifically, for Anti-Tank Guided Missiles (ATGM) that attack ground targets, the effectiveness of the terminal guidance law is essential. It must achieve high accuracy and adhere to specific impact angle constraints. The need for impact angle constraints in ATGMs' terminal guidance laws arises from two primary reasons. First, these constraints allow the missile to hit the tank at its weakest point typically the top, where the armour is thinner and more vulnerable. This tactic enhances the missile's combat effectiveness without needing larger or heavier warheads. By implementing a guidance law that constrains the impact angle, modern ATGM systems enable the missile to carry out a "top-attack" mode, significantly improving its capability to damage or destroy the target.

Second, tanks often come equipped with active defence systems designed to counter attacks from the front or other predictable angles. ATGM with impact angle constraints can strike from less defended angles, thereby boosting their ability to penetrate the tank's armour and destroy the target effectively. This feature is crucial for modern anti-tank warfare, making impact angle constraints an essential aspect of ATGM guidance law design.

The synthesis of Impact Angle Control Guidance (IACG) laws has been studied by many authors over the decades. Previous works can be categorized into the following methods: optimal control approaches [2–6], Proportional Navigation Guidance (PNG) approaches [7–9], Sliding Mode Control (SMC) approaches [10, 11], backstepping control approaches [12, 13], and other methods. The State-Dependent Riccati Equation (SDRE) technique is used to synthesize a guidance law with impact angle constraints [13], enabling precise control of the impact angle for ATGM targeting stationary objects. Kim *et al.* [14] proposes fixed-time convergent error dynamics for the design of guidance laws, particularly for impact angle control. This method improves system performance and ensures convergence before impact with high accuracy.

Although guidance laws with considerable impact angle constraints offer many benefits, especially for ATGM by

Manuscript received April 30, 2024; revised July 5, 2024; accepted July 11, 2024; published January 17, 2025.

maximizing the warhead's combat effectiveness, they tend to create highly curved missile trajectories. With such trajectories, the variation in the look angle from strap-down seekers with a narrow Field of View (FOV) can exceed the allowable FOV limits, leading to the risk of losing target information. The FOV constraint refers to the limitations on the angular range within which a missile's seeker or sensor can effectively detect and track a target.

When the missile transitions to the terminal guidance phase, it is crucial to maintain target lock throughout this process. This means the guidance law must ensure that the line of sight between the missile and the target always remains within the seeker's FOV limits. Therefore, guidance laws considering the FOV limit [4, 6, 11, 14–20] have been recently proposed. For further analysis, existing studies related to IACG with FOV constraints can be classified into two approaches based on the target dynamics: guidance laws designed exclusively for stationary targets [14, 16, 19, 20] and guidance laws capable of handling moving targets [4, 15, 17, 18].

The problem of handling the FOV constraint of the seeker in existing guidance laws often employs a general optimal control method with an inequality constraint on the state variable related to the FOV [4, 6]. Some guidance laws use sliding mode control, applying a sigmoid function for the FOV constraint, which has been implemented for stationary targets in [14] and extended to moving targets in Ref. [17].

In existing guidance laws, we have identified several issues that need addressing. Specifically, linear methods often assume small angles, whereas in reality, the flight path angle of missiles tend to become large, especially requiring constraints on large impact angles. This can reduce guidance accuracy and lead to significant miss distances.

Using backstepping control, SMC methods can effectively tackle nonlinear problems, a challenge often encountered in optimal control theory. Although these guidance commands usually demonstrate effectiveness in nonlinear scenarios, nonlinear guidance laws typically cannot provide optimality based on any specific quality index. Therefore, understanding their physical workings can be challenging.

The guidance laws based on SMC, due to frequent utilization of switching logic, render the command acceleration discontinuous, significantly diminishing its theoretical value. Moreover, the behaviour of errors in heading and impact angles, and the role of guidance gains in reducing these errors, remains unclear.

The proposed guidance law in Ref. [20] addresses both impact angle and FOV constraints while reducing sensitivity to initial guidance errors. It achieves the desired impact angle error behavior by utilizing optimal error dynamics. However, this paper only tackles the fixed target scenario.

Developing the guidance problem in [20] to extend its application to moving tank targets encounters significant challenges in estimating the missile's terminal flight path angle, leading to difficulties in determining the impact angle error. Since the estimated flight path angle at the final time depends on many variables when the target is moving, the problem becomes more complex. To address this, in this paper, we propose a new guidance law to control the impact angle while considering the field of view constraints of the seeker. This law targets explicitly non-maneuvering moving tanks using a nonlinear virtual relative reference frame.

The basic nonlinear virtual relative model transforms the problem of tracking and intercepting a moving target by redefining the dynamics of both the missile and the target in a virtual reference frame. This reference frame is typically chosen to move along with the target, with the origin attached to the target, thereby simplifying the mathematical model describing the missile's motion and the target in this coordinate system. This transformation converts the problem of synthesizing guidance laws for a constant-velocity missile attacking a moving target into the problem of synthesizing guidance laws for a variable-velocity missile attacking a stationary target [21].

Using the method of designing guidance laws based on optimal error dynamics [20] for the fixed-target problem in the virtual reference coordinate system with approach angle constraints.

After synthesizing the guidance law in the virtual reference coordinate system, the required guidance laws in the inertial coordinate system will be derived.

A suitable weighting function is introduced to enhance command acceleration distribution in the terminal homing phase. This aims to minimize initial guidance command requirements and gradually reduce the magnitude of guidance commands to zero as the terminal time approaches.

Furthermore, the guidance law is refined by incorporating a saturation function to efficiently address the seeker's maximum FOV angle constraint.

II. Problem Statement

A. Engagement Kinematics

Within the scope of this paper, we only consider the movement of a tank target along the X-axis in the missile's trajectory plane. The planar homing guidance scenario is depicted in Fig. 1, where a missile with a narrow FOV is engaged against a non-maneuvering incoming target. In the Cartesian inertial reference frame X_IOY_I, the subscripts $\boldsymbol{M}$, and $\boldsymbol{T}$ refer to the missile and the target, respectively. The symbols in Fig. 1 include:

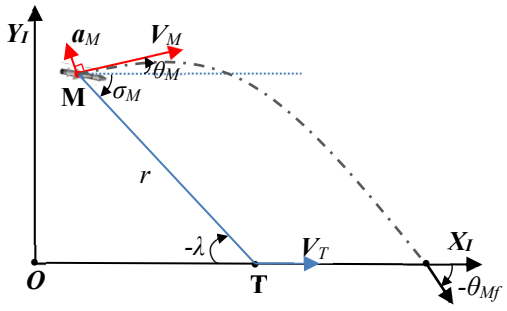

Fig. 1. Two-dimensional homing engagement geometry in the inertial coordinate system.

where r indicate the relative distance between the missile and the target; V_M ; V_T indicate velocity vectors of the missile and target; $\boldsymbol{a_M}$ indicate the acceleration vector of the missile, applied perpendicular to V_M; θ_M indicate the flight-path angle of the missile; λ indicate the Line-of-Sight (LOS) angle; σ_M indicate the look angle of the seeker, assuming the missile's angle of attack is small enough to be neglected; θ_{Mf} indicate the missile's flight-path angle at the moment of interception.

Since we are considering a target tank moving on the ground, restricted to motion in the vertical plane, the lateral acceleration command perpendicular to the target is $a_T = 0$. The positive direction for angles is counterclockwise.

The nonlinear engagement geometry in the X_IOY_I frame is constructed as follows:

$$\dot{r} = V_T\, cos(\theta_T - \lambda) - V_M\, cos(\theta_M - \lambda) \quad (1)$$

$$\dot{\lambda} r = V_T\, sin(\theta_T - \lambda) - V_M\, sin(\theta_M - \lambda) \quad (2)$$

$$\dot{\theta}_M = \frac{a_M}{V_M} \quad (3)$$

$$\dot{\sigma}_M = \dot{\theta}_M - \dot{\lambda} \quad (4)$$

As depicted in Fig. 1, the impact angle θ_{imp} is the angle between the missile's and target's velocity vectors at the moment of interception and is determined by:

$$\theta_{imp} = \theta_{Mf} - \theta_{Tf} \quad (5)$$

Because the target is a tank that only moves on the ground, the flight-path angle of the target is $\theta_T = \pi$ when the target is approaching and $\theta_T = 0$ when the target is receding.

Traditional methods for solving the optimal guidance problem with angle constraints typically start by linearizing the nonlinear kinematic equations under the small-angle assumption. Analytical solutions are then derived using optimal control theory. However, the trajectory of guidance laws with considerable impact angle constraints is highly curved, making the small-angle assumption inaccurate and reducing the performance of linear optimal guidance laws. To address this issue, we use a reference frame to transform the original problem into an equivalent one, deriving optimal guidance solutions without linearization.

Fig. 2 illustrates the kinematics of relative engagement and the geometric relationship between vectors in both coordinate frames.

The notation $X_RO_RY_R$ represents the relative coordinate system attached to the target, with the origin at the target itself. The variables V_R and θ_R represent the relative speed and relative flight path angle, respectively. The relative lead angle is denoted by σ_R, calculated as the difference between θ_R and σ. The symbol a_R represents the component of the relative acceleration perpendicular to the relative velocity vector $\boldsymbol{V_R}$. The relative velocity vector $\boldsymbol{V_R}$ is defined as the difference between the missile velocity $\boldsymbol{V_R}$ and the target velocity $\boldsymbol{V_R}$.

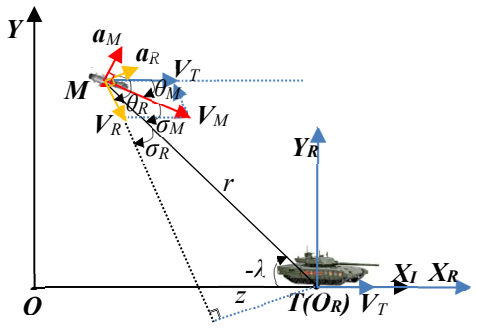

Fig. 2. The geometric relationship between vectors.

The relative velocity and relative flight path angle of the missile can be determined based on the geometric relationship shown in Fig. 2 as follows [21].

$$V_R = \sqrt{V_M^2 + V_T^2 - 2V_M V_T \cos(\theta_M - \theta_T)} \quad (6)$$

$$\theta_R = \tan^{-1} \frac{\sin\theta_M - \eta \sin\theta_T}{\cos\theta_M - \eta \cos\theta_T} \quad (7)$$

$$\eta = {}^{V_T}/_{V_M} \quad (8)$$

In the $X_RO_RY_R$ reference frame shown in Fig. 2, the differential equations describing the motion and dynamic geometric correlation between the missile and the target are as follows:

$$\dot{r} = -V_R \cos\sigma_R \quad (9)$$

$$\dot{\lambda} = \frac{-V_R \sin\sigma_R}{r} \quad (10)$$

$$\dot{\theta}_R = \frac{a_R}{V_R} \quad (11)$$

$$\dot{\sigma}_R = \dot{\theta}_R - \dot{\lambda} \quad (12)$$

$$\dot{V}_R = -a_R \tan(\theta_M - \theta_R) \quad (13)$$

$$a_R = a_M \cos(\theta_M - \theta_R) \quad (14)$$

$$\theta_M - \theta_R = \cos^{-1}\left(\frac{1-\eta^2+V_R^2/V_M^2}{2V_R/V_M}\right) \quad (15)$$

In this context, we consider a_R as a control parameter. Additionally, it can be inferred from the geometric configuration in Fig. 2 and Eq. (6) that V_R varies with time, is positive, and is bounded by the following expression:

$$\begin{cases} V_R(t) \geq (1-\eta)V_M > 0 \\ V_R(t) \leq (1+\eta)V_M \end{cases} \quad (16)$$

Therefore, in the nonlinear relative coordinate system, the original problem of a missile with constant velocity intercepting a non-maneuvering moving tank becomes a problem of a missile with varying velocity facing a stationary target. The significant advantage of this

transformation is that we can formulate and solve the guidance problem without the need for linearization.

B. Problem Formulation

Before we delve into the problem formulation, let's explain the fundamental concept related to the paper: Zero-Effort-Miss (ZEM).

The ZEM is defined as the distance between the missile and the target if the target maintains its current trajectory and the missile takes no additional corrective maneuvers [22]. In the reference frame depicted in Fig. 2, the Zero-Effort-Miss (ZEM), represented by z, can be expressed as:

$$z = -r \sin \sigma_R \tag{17}$$

The primary objective of the guidance law designed in this paper is to control the impact angle of the ATGM when engaging non-maneuvering moving tanks, considering the missile's seeker's Field of View (FOV) limitations. The guidance law ensures the missile hits the target at a specified impact angle, enhancing the warhead's effectiveness, particularly for a "top-attack" mode that targets the turret area where the armor is thinnest. Additionally, the guidance law optimizes command acceleration during the terminal homing phase, minimizes initial guidance command requirements, and reduces the guidance command to near zero at the terminal time.

The purpose of the synthesized guidance law is to strike the target at the desired impact angle θ_{fd}, maintain target lock-on by ensuring the seeker's angle of view does not exceed the maximum permissible value σ_{max}, and distribute command acceleration reasonably throughout the flight. This is achieved by satisfying the constraints mathematically described in Eqs. (18)–(21).

$$z(t_f) = 0 \tag{18}$$

$$\theta_{imp} \to \theta_{fd} \; as \; t \longrightarrow t_f \tag{19}$$

$$|\sigma| \leq \; \sigma_{max} < \frac{\pi}{2}, \forall t \in [t_0, t_f] \tag{20}$$

$$\begin{cases} a_M(t_0) \\ a_M(t_f) \end{cases} small \tag{21}$$

where t_0 is the initial time and t_f is the interception time.

From Eq. (10) and Eq. (18), it follows that to successfully intercept the target, $\sigma_R(t_f) = 0$. In this case, Eq. (18) is equivalent to:

$$\theta_{Rf} = \lambda_f \tag{22}$$

When the missile and the target are on a collision course, a unique LOS angle will correspond to each impact angle. The missile's lateral acceleration directly influences the change in the LOS angle. This indicates that we can calculate the necessary command acceleration to achieve the desired impact angle by expressing the impact angle as a function of the LOS angle. The one-to-one correspondence relationship between the impact angle θ_{imp} and the final line-of-sight angle λ_f can be determined from Eq. (2) when successfully approaching the target at the terminal time as follows:

$$V_T \, sin(\theta_{Tf} - \lambda_f) = V_M \, sin(\theta_{Mf} - \lambda_f) \tag{23}$$

Combining Eq. (5), the Eq. (23) can be re-expressed as follows:

$$sin(\theta_{Tf} - \lambda_f + \theta_{imp}) = \eta \, sin(\theta_{Tf} - \lambda_f) \tag{24}$$

Because $\eta < 1$ and the θ_T angle is always fixed ($\theta_T = 0$ or $\theta_T = \pi$). Using the difference formula for sines for the left-hand side and then proceeding through some simple transformations, we obtain the λ_f angle. It is important to note that the collision triangle condition in Eq. (24) can be satisfied by two different geometric configurations. The final LOS angle can be classified according to the target's relative direction to the missile as follows [23]:

$$\lambda_f = \begin{cases} \theta_T - tan^{-1} \frac{sin \, \theta_{imp}}{cos \, \theta_{imp} - \eta} \; if \; |\theta_T - \theta_M| < \pi/2; \\ \theta_T - \pi - tan^{-1} \frac{sin \, \theta_{imp}}{cos \, \theta_{imp} - \eta} \; if \; |\theta_T - \theta_M| > \pi/2; \end{cases} \tag{25}$$

From Eqs. (22) and (25), it is evident that the desired impact angle constraint at the final time can be satisfied by controlling the terminal relative flight path angle. In that case, the desired terminal relative flight path angle θ_{Rd} can be determined easily as follows:

$$\theta_{Rd} = \begin{cases} \theta_T - tan^{-1} \frac{sin \, \theta_{fd}}{cos \, \theta_{fd} - \eta} & \text{if Receding Target} \\ \theta_T - \pi - tan^{-1} \frac{sin \, \theta_{fd}}{cos \, \theta_{fd} - \eta} & \text{if Approaching Target} \end{cases} \tag{26}$$

This subsequently reveals that the constraint on the impact angle in Eq. (19) is equivalent to the constraint on the terminal relative flight path angle as follows:

$$\theta_R(t_f) = \theta_{Rd} \tag{27}$$

C. The Concept of Optimal Error Dynamics

Designing guidance laws tackles a control problem aimed at monitoring and adjusting errors within a finite period. Defining the relevant guidance error, denoted as *e(t)*, is crucial for achieving the intercept condition. In order to establish the system equations describing the dynamics of the selected guidance error, we derive the guidance error's derivative over time. This derived equation illustrates the variation of the guidance errors over time and provides insights into their behavior and attributes. The general form of the system equation is as follows:

$$\dot{e}(t) = g(t)u(t) \tag{28}$$

where *e(t)* indicates the tracking error; *g(t)* indicate a specified time-dependent function.

Depending on the specific guidance problem, the corresponding function $g(t)$ can be determined. This function is invertible because the tracking problem is controllable, meaning $g(t) \neq 0$, while $u(t)$ is the control input of the system. He *et al.* [16] provided a summary of the Error Dynamics method and introduced the Optimal Error Dynamics (OED) method. Moreover, they formulated the OED equation as follows:

$$\dot{e}(t) + \frac{\rho(t)}{t_{go}} e(t) = 0 \tag{29}$$

where $t_{go} \triangleq t_f - t$ denotes the time-to-go, indicating the missile's remaining flight time until the target is intercepted. Eq. (29) is a simple form of Cauchy-Euler type differential equation. The analytical solution of the Eq. (29) takes the following form:

$$e(t) = e(t_0)\left(\frac{t_{go}}{t_f}\right)^{\rho} \tag{30}$$

From Eq. (30), it can be seen that if $e(t_0)$ is initially non-zero, the error $e(t)$ will approach zero as t_{go} gradually approaches zero. Where $\rho > 0$ is the gain that changes over time, characterizing the rate at which the error $e(t)$ converges to zero and is determined as follows:

$$\rho(t) = \frac{t_{go} W^{-1}(t) g^2(t)}{\int_t^{t_f} W^{-1}(\tau) g^2(\tau) d\tau} \tag{31}$$

where, $W(t) > 0$ is called the weighting function with arbitrary forms but must always be positive. The control input resulting from the OED method described above minimizes the cost function specified below. The full proof, utilizing the Schwarz inequality theorem, has been detailed in [16].

$$J = \frac{1}{2}\int_t^{t_f} W(\tau) u^2(\tau) d\tau \tag{32}$$

III. Guidance Law Design

A. Derivation of IACG Against A Moving Target

In this section, the impact angle control guidance law will be initially designed based on prediction-correction guidance principles. Utilizing the expression of the derived guidance law, the subsequent step involves designing a weighting function to shape the acceleration command to meet the requirements specified in constraint (21). Lastly, resolving the seeker's FOV constraint is necessary to ensure satisfaction of condition (20).

The guidance law command is formulated as a combination of two components:

$$a_R = a_{R0} + a_{RB} \tag{33}$$

where, a_{R0} represents the base command intended to ensure zero ZEM for target interception, while a_{RB} is the correction component aimed at meeting the condition of the impact angle.

By employing the standard optimal control theory as explicitly presented and demonstrated in the paper [21], the guidance law ensuring zero ZEM for target interception is formulated as follows.

$$a_{R0} = NV_R\dot{\lambda} \tag{34}$$

The guidance law (34) synthesized in the reference frame has the same form as the ideal PNG: $a_{R0} = a_{R,PNG}$ [24]. However, in the above expression, the variable V_M is replaced by the variable V_R.

To explain the physical significance of the Relative Proportional Navigation Guidance (RPNG), we rephrase related terms as follows to make them more understandable. Substituting Eq. (10) into (34), we obtain the guidance law expression as:

$$a_{R,PNG} = -\frac{NV_R \sin\sigma_R}{\frac{r}{V_R}} \tag{35}$$

The guidance law is applied in the terminal homing phase with a strap-down seeker configuration, so the virtual look angle σ_R is relatively small. Hence, it can be approximated that $\sin\sigma_R \approx \sigma_R$. And the time to go is approximately calculated as follows: $t_{go} \approx r/V_R$. In this case, Eq. (35) can be rewritten as follows:

$$a_{R,PNG} = \frac{NV_R e_h}{t_{go}} \tag{36}$$

From Eq. (36), $e_h = \lambda - \theta_R = -\sigma_R$ can be described as the heading angle error for a virtual fixed target in the reference coordinate system $X_R O_R Y_R$. Therefore, this term functions as a feedback control command that adjusts the heading angle error using a proportional gain that varies with time. Its purpose is to maintain $\theta_R = \lambda$.

Next, we'll examine the command acceleration term a_{RB}. When the condition of $a_{RB} = 0$, the optimal guidance command becomes the base RPNG law as $a_R = a_{R,PNG}$. We will determine the desired relative terminal flight-path angle from the impact angle constraint Eq. (19), substituting into Eq. (26). Following the method of deriving guidance laws as mentioned above, considering in the relative reference frame, the command acceleration component a_{RB} will be designed to adjust the error between $\hat{\theta}_{Rf}$ and θ_{Rd} to zero.

Substituting Eq. (34) into Eq. (11), we obtain the dynamics of the relative flight-path angle as follows:

$$\dot{\theta}_R = N\dot{\lambda} \tag{37}$$

Integrating both sides of Eq. (37) over the interval from t to t_f, and then combining with Eq. (22), the final relative flight-path angle adjusted by the base guidance law Eq. (36) can be predicted as

$$\hat{\theta}_{Rf} = \frac{N}{N-1}\lambda - \frac{1}{N-1}\theta_R \tag{38}$$

Eq. (38) calculates the relative flight path angle achieved at the final time in the nonlinear virtual relative model when using PNG law with a navigation constant *N*. where, $e_{\theta f} \triangleq \theta_{Rd} - \hat{\theta}_{Rf}$ represents the predicted angular error by the expression of the base guidance law in Eq. (34). Then, the time derivative of $e_{\theta f}$ is:

$$\dot{e}_{\theta f} = -\frac{N}{N-1}\dot{\lambda} + \frac{1}{N-1}\dot{\theta}_R = -\frac{N}{N-1}\dot{\lambda} + \frac{1}{N-1}\frac{a_R}{V_R} \tag{39}$$

Substituting Eq. (33) into Eq. (39), we obtain:

$$\dot{e}_{\theta f} = \frac{1}{N-1}\frac{a_{RB}}{V_R} \tag{40}$$

In this case, from Eq. (28), the functions *g(t)* and the control input signal *u(t)* are obtained in the following forms.

$$\begin{cases} g(t) = \frac{1}{(N-1)V_R} \\ u(t) = a_{RB} \end{cases} \tag{41}$$

To ensure the angular error converges to zero at the final time, we adopt the following optimal error dynamics:

$$\dot{e}_{\theta f} + \frac{k}{t_{go}} e_{\theta f} = 0 \tag{42}$$

By substituting Eq. (40) into Eq. (42), the biased guidance command a_{RB} is expressed as follows:

$$a_{RB} = -\frac{k(N-1)V_R}{t_{go}} e_{\theta f} \tag{43}$$

From the guidance law expression Eq. (43), we can observe that the physical significance of a_{RB} can be interpreted as a control command that adjusts the impact angle error using the predictor-corrector method. In the guidance law expression Eq. (43), k is the tuning coefficient that determines the convergence rate of the impact angle error, and the larger this coefficient, the faster the convergence rate of the predicted angular error to zero. Therefore, the synthesized guidance law, when described in the virtual reference frame, is derived as follows:

$$a_R = NV_R\dot{\lambda} - \frac{k(N-1)V_R}{t_{go}} e_{\theta f} = \frac{NV_R e_h}{t_{go}} - \frac{k(N-1)V_R}{t_{go}} e_{\theta f} \tag{44}$$

Then, by substituting Eq. (44) into Eq. (14), we obtain the IACG law in the inertial coordinate system as follows:

$$a_M = \frac{a_R}{cos(\theta_R - \theta_M)} \tag{45}$$

Fig. 3 illustrates the block diagram depicting the operational principle of the IACG with a Non-maneuvering moving target based on the optimal error dynamics method and the nonlinear virtual relative model. The guidance law Eq. (44) encounters difficulty when applied in the terminal homing phase of ATGM, as the initial guidance command requirement is very large, leading to the possibility of command saturation. This primarily arises from the a_{RB} component for the following reasons.

The terminal guidance phase of ATGM typically has a short duration (small t_{go}), with the 'top attack' capability leading to a large initial predicted angle error $e_{\theta f}$. Meanwhile, the a_{RB} component is susceptible to the significant initial value of $e_{\theta f}$ and the small t_{go}, requiring a considerable acceleration command at the initial homing phase to meet that demand.

On the other hand, the initial acceleration command component $a_{R,PNG}$, tends to be relatively small. This is because, during the midcourse phase, the guidance law of this phase aims to minimize the gap between the flight path angle and the look angle at the initiation of the terminal homing phase, particularly for ATGMs equipped with a strap-down seeker having a limited FOV. Therefore, at the inception of the terminal homing phase, the initial heading angle error e_h is relatively small, resulting in the command acceleration component $a_{R,PNG}$ also being small initially.

This paper proposes using a suitable weighting function *W(t)* to address the mentioned drawback and optimize the distribution of the a_{RB} acceleration command term during the terminal homing phase. The goal is to minimize the initial guidance command requirements and approach zero magnitudes of the guidance command by the final time.

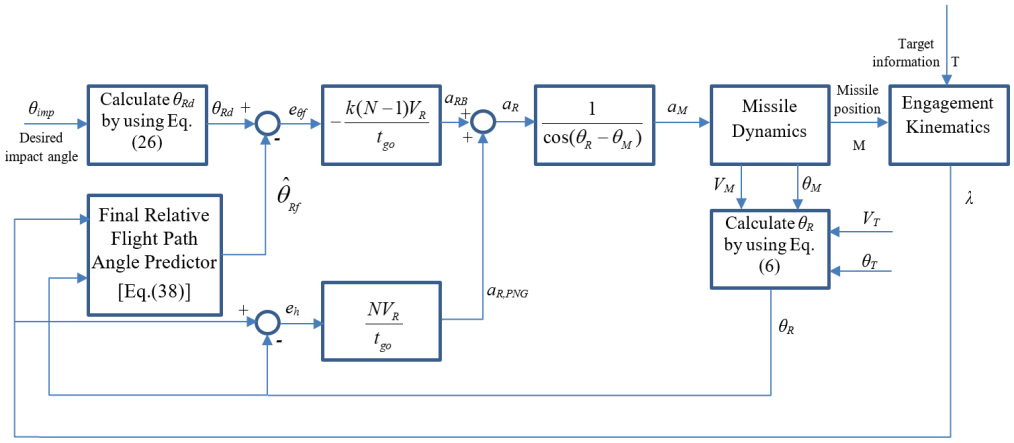

Fig. 3. Block diagram depicting the fundamental operation of IACG law with non-maneuvering moving target.

B. Design of the Weighting Function

The previous presentation on the theoretical foundation for optimal error dynamics showed that the weighting function $W(t)$ plays a crucial role in determining the value of the guidance command. An arbitrary weighting function $W(t) > 0$ determines the shape of the optimal control signal. When the value of the weighting function $W(t)$ is relatively large, the magnitude of the control signal will decrease to minimize the performance index Eq. (32). Therefore, increasing the relative weighting at both the beginning and end of the terminal homing phase will reduce the initial and final command accelerations compared to the case of evenly distributed relative weighting throughout the engagement process. Thus, distributing the value of this weighting function throughout the engagement process makes it feasible to adjust the command acceleration.

Once the appropriate weighting function is selected, we derive the expression of the adjustment coefficient function $k(t)$ from Eq. (31) as follows

$$k(t) = \frac{t_{go} W^{-1}(t) g^2(t)}{\int_t^{t_f} W^{-1}(\tau) g^2(\tau) d\tau} \tag{46}$$

We can assume without loss of generality that the function $g(t)$ is a constant. In this scenario, we aim to select the weighting function $W(t) = g^2(t)R(t)$ in order to ensure that the coefficient $k(t)$ in the integration calculation in Eq. (46) is independent of the function $g(t)$. The objective of designing this weighting function is to modify the amplitude of the guidance command by altering the value of the weighting function over time. To put this concept into practice, our study proposes a function $R(t)$ in the form of a second-order polynomial:

$$R(t) = \frac{a(t_{go}-b)^2}{t_{go}} + \frac{1}{t_{go}} \tag{47}$$

The equation above suggests that the variables $a > 0$ and $b > 0$ serve as distribution parameters for designing the weighting function. The weighting function $W(t)$ has a higher or minimum values at specific points in the engagement process than other points. To optimize the cost function J in Eq. (32), the system must maximize or minimize the guidance commands at these points accordingly. This approach allows designers to fine-tune the guidance command profile throughout the homing guidance phase by adjusting the parameters a and b.

Unlike traditional PNG with constant weighting corresponding to a fixed gain factor or some guidance laws with monotonically increasing weight functions on the cost function [3, 6], the proposed method can generate a non-monotonic weight function that may have extreme points.

From Eq. (47), it is clear that the weighting function $R(t)$ has its minimum value at $t_{go} = \sqrt{b^2 + 1/a}$ and its maximum value at the interception point ($t_{go} = 0$). The simulation results in Fig. 4 show that choosing suitable design parameters a and b makes it easy to distribute the relative weighting throughout the engagement process, including the minimum and maximum values and the ratio of initial and final values to the minimum value. In contrast, a weighting function in the form of $1/t_{go}$ starts at zero initially and then monotonically increases throughout the cost function.

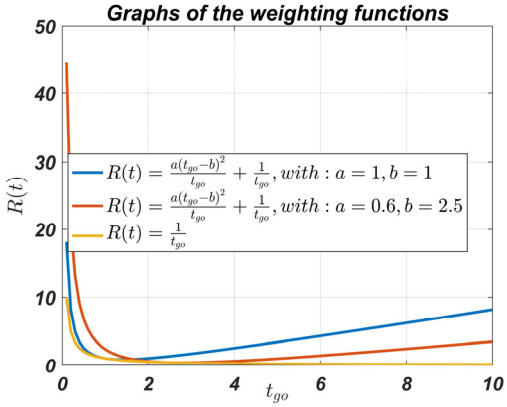

Fig. 4. Compare the weighting functions and the effects of the design parameters a and b.

For several reasons, the proposed weighting function is designed to minimize guidance commands at the beginning and end of the missile's trajectory. Large initial commands can lead to command saturation, abrupt trajectory changes, and potential instability. Reducing initial guidance commands ensures a smoother transition from the midcourse phase to the terminal homing phase, enhancing system stability. In practical scenarios, lateral acceleration is constrained by aerodynamic limits. Minimizing terminal command acceleration reduces the likelihood of command saturation near the target, thus improving missile performance. Maintaining a low terminal command acceleration also results in a smaller attack angle at impact, which is crucial for maximizing the warhead's effectiveness in ATGM systems.

By substituting Eq. (47) into Eq. (46), we can express $k(t)$ as follows:

$$k(t) = \left(\frac{2at_{go}^2}{a(t_{go}-b)^2+1}\right)\left(\frac{1}{ln\left(\frac{1+a(t_{go}-b)^2}{1+ab^2}\right)+2\sqrt{a}b\,tan^{-1}\left(\frac{\sqrt{a}t_{go}}{1-ab(t_{go}-b)}\right)}\right) \tag{48}$$

C. Derivation of IACG Against A Moving Target with FOV Constraint

The developed guidance law uses a nonlinear function to keep the velocity lead angle within the seeker's FOV constraint. Let $\Phi(x)$ be the user-defined nonlinear function shaping the velocity lead angle. This function, defined on the interval [−1,1], must satisfy the following properties: $\Phi(-1) = \Phi(1) = 0$ and $\Phi(0) = 1$. Additionally, $\Phi(x)$ must monotonically increase for $x \in [-1, 0]$ and monotonically decrease for $x \in (0, 1]$. There are various forms of the function $\Phi(x)$ that satisfy the conditions mentioned in [16]. We have chosen a specific candidate function with the following form.

$$\Phi(x) = \frac{1}{2}cos(\pi x^n) + \frac{1}{2} \tag{49}$$

where, $n > 0$ is a design parameter used to regulate the curvature of $\Phi(x)$. Fig. 5 illustrates the plots of the candidate function corresponding to different values of the parameter n.

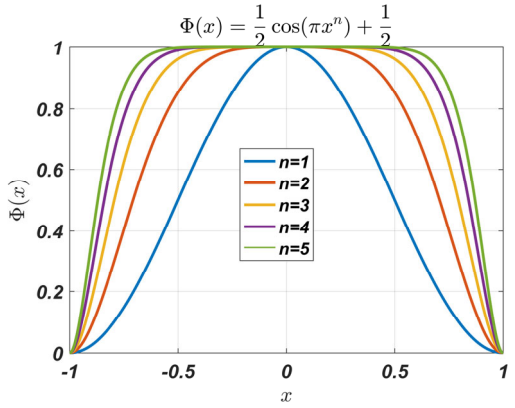

Fig. 5. Profiles of the $\Phi(x)$ function with different n.

With larger values of n, $\Phi(x)$ approaches 1 when $|x| < 1$ and rapidly converges to zero as $|x|$ approaches 1. Therefore, n serves as a design trade-off between the desired impact angle and the velocity lead angle limit: a higher n value allows for a longer adjustment time for the desired impact angle. A lower n value maintains more adjustment time for the velocity look angle.

When the variable x of the nonlinear function is expressed as σ/σ_{max}, it allows for adjusting the feedback guidance command based on the impact angle error: corrective intervention decreases as the look angle σ nears its maximum permissible value σ_{max}. If $\sigma = \sigma_{max}$, the guidance law transitions into a PNG law. It's worth noting that even when the proposed law becomes RPNG, it continues to satisfy the Field-of-View (FOV) constraint since the virtual look angle σ in the RPNG always gradually decreases for a virtual stationary target [23]. Combining Eqs. (44), (48), and (49), we have the expression of the impact angle constrained guidance law considering the FOV limit and the weighting function in the reference coordinate system $X_R O_R Y_R$ as follows:

$$a_R = NV_R\dot{\lambda} - \frac{k(N-1)\Phi\left(\frac{\sigma}{\sigma_{max}}\right)V_R}{t_{go}} e_{\theta f} = \frac{NV_R e_h}{t_{go}} - \frac{k(N-1)\Phi\left(\frac{\sigma}{\sigma_{max}}\right)V_R}{t_{go}} e_{\theta f} \quad (50)$$

The guidance law expression Eq. (50) can be understood as a linear combination of feedback control commands for heading angle error and predicted angular error, enhancing noise resistance and robustness to changes in missile velocity. To implement the guidance law Eq. (50), we need to provide information beyond the predetermined design parameter values. This includes parameters such as angles λ and σ, the LOS rate, range r, V_M, V_T, and the parameter t_{go}. These values result from transformations of quantities like V_R and $e_{\theta f}$ to the original parameters in Eqs. (15) and (26), etc.

The angles λ and σ, along with V_M, are measured by the integrated strap-down image seeker and the Inertial Navigation System (INS). Additionally, the LOS rate estimated by the extended Kalman filter within the seeker system has been studied in many research works [25]. The relative distance estimation method uses infrared imaging information measured from the number of target pixels on the imaging plane. By relating the pixel count of the image to the actual size of the target, the relative distance between the missile and the target is calculated [26]. The desired impact angle $\theta_{imp} = \theta_{fd}$ is predetermined. Thus, missiles equipped with seeker and INS can implement the proposed guidance law.

Implementing IACG necessitates the knowledge of the time-to-go. Since no devices directly measure this parameter, it must be estimated based on available information.

D. Estimation Time to Go

The parameter t_{go}, defined as the remaining flight time $t_{go} = t_f - t$, is crucial for linking relative velocity to the desired impact angle. For practical purposes, this paper uses an efficient method to estimate t_{go} for impact angle control. To intercept the target, the final time of the virtual look angle approaches zero ($\sigma_R = 0$). This implies that from Eq. (9), we have the final closing velocity equal to the terminal relative speed as $V_{Cf} = V_{Rf}$.

$$V_{Rf} = \sqrt{V_M^2 + V_T^2 - 2V_M V_T \cos(\theta_{imp})} \quad (51)$$

In that case, the average closing velocity can be approximated as follows:

$$\bar{V}_C = mV_R \cos\sigma_R + (1-m)V_{Rf} \quad (52)$$

The coefficient $m \in [0, 1]$ is chosen by the user, depending on the profile form of the closing velocity. Selecting $m = 0.5$ is considered the simplest option. Hence, the estimation of time-to-go can be derived as:

$$t_{go} \approx \frac{r}{\bar{V}_C} \quad (53)$$

IV. Numerical Simulations

This section presents the performance of the proposed guidance laws through three subsections of nonlinear simulations:

- **Scenario 1**: Varying impact angles with fixed Field-of-View (FOV).

Nonlinear simulations are conducted with varying impact angles while keeping the FOV of the seeker fixed. This scenario aims to study the feasibility of implementing IACG.

- **Scenario 2**: Different FOV Limits with Fixed Impact Angles.

Simulations are carried out with different FOV limits and fixed impact angles. This scenario evaluates the effectiveness of the guidance law in handling various FOV constraints.

- **Scenario 3**: Weighting Function Application.

Simulations are performed for the guidance law with and without applying the weighting function $W(t)$. This scenario assesses the effectiveness of the weighting function. It also compares it with the previously studied extended Trajectory Shaping Guidance (TSG). Nonlinear

simulations are conducted using a realistic ATGM model applied to the terminal homing phase in head-on and tail-chase engagement scenarios. It is assumed that all necessary information can be obtained without noise and that the missile operates without delay or command saturation.

In the guided missile model with commanded acceleration generated by aerodynamic forces, the missile's velocity and flight path angle are assumed to change as follows, considering the effects of aerodynamic forces, gravitational forces, and engine thrust. In the aerodynamic guided missile model, assuming that during the terminal guidance phase, the missile's thrust-producing propulsion system has stopped operating and no longer affects the missile's speed, disregarding disturbances caused by longitudinal wind gusts. Therefore, considering both aerodynamic and gravitational forces, the missile's velocity and flight path angle are assumed to vary as follows:

$$\dot{V}_M = -\frac{D}{m} - g\sin\theta \tag{54}$$

$$\dot{\theta}_M = \frac{a_M - g\cos\theta}{V_M} \tag{55}$$

where D, m, and g represent the aerodynamic drag, missile mass, and acceleration of gravity, respectively. The drag model used in [26, 27] is applied to construct D in our simulation.

$$D = C_{D0} Q S_{ref} + \frac{K_i m^2 a_M^2}{Q S_{ref}} \tag{56}$$

where, C_{D0} indicate the zero-lift drag coefficient; Q indicate dynamic pressure; S_{ref} indicate Reference area; K_i indicate the induced drag coefficient.

The values of these parameters are chosen to be suitable for antitank missiles as described specifically in [27, 28].

A. Simulation Setup

To conduct the simulation, we use the derived guidance law a_M to solve the differential equations involving state variables such as the relative distance between the missile and the target, the line-of-sight angle, the missile flight path angle, the seeker's look angle, the missile velocity, the missile position coordinates, the target flight path angle, and the target position coordinates.

The parameters and initial state variables are provided in Table I, with some initial states easily calculated from the given values. The ODE45 solver in Matlab is used to integrate these differential equations over time. An event function terminates the simulation when the missile's altitude reaches 2 m in all the scenarios, corresponding to the estimated height of the tank.

The initial coordinates of the missile and target are set according to the maximum detection range of the missile's seeker and the handover point transitioning from the midcourse phase to the terminal guidance phase. For modern tanks, the maximum speed can reach up to 80–90 km/h, such as the T-14 Armata tank [29]. In the simulations, we are testing an extreme situation where the target moves uniformly along the X-axis at a maximum speed of 25 m/s. The parameters for designing the weighting function in the simulations are chosen fixed as follows: $a = 0.5$ and $b = 2.5$. The guidance coefficient N is set to 3, and other parameters, such as the desired impact angle and the seeker's field of view limits, are chosen according to each specific scenario in the corresponding subsections.

TABLE I. THE SIMULATION CONDITIONS

Parameter	Value
Missile initial position (x_{M0}, y_{M0})	(0, 400) m
Missile initial velocity V_{M0}	250 m/s
Initial lead angle (σ_0)	10°
Initial relative distance (r_0)	$\sqrt{(x_{T0}-x_{M0})^2+(y_{T0}-y_{M0})^2}$
Initial LOS angle (λ_0)	$tan^{-1}\left(\frac{(y_{T0}-y_{M0})}{(x_{T0}-x_{M0})}\right)$
Initial missile path flight angle (θ_{M0})	$(\sigma_0 + \lambda_0)$ (deg)
Initial target position (x_{T0}, y_{T0})	(1200, 0) m for head-on case (1000, 0) m for tail-chase case
Target velocity V_T	25 m/s
The direction of the target $\theta_T = \theta_{T0}$	0° for head-on case or 180° for tail-chase case

1) Scenario 1

First scenario addresses attacks on non- maneuvering moving tanks with constraints on different impact angles of 50°, 70°, 80°, 90°, and a fixed field of view limit of σ_{max}=25°, and other initial conditions taken from Table I for the head-on engagement case.

The simulation results, as shown in Fig. 6, illustrate the effectiveness of the synthesized guidance law in meeting these constraints. Fig. 6(a) and (b) demonstrate that the proposed guidance law enables the missile to hit the target at the specified impact angles for a moving tank traveling at a constant velocity in all cases. Specifically, Fig. 6(a) shows that achieving a larger impact angle necessitates a longer and more curved missile trajectory. In Fig. 6(c) and Fig. 6(e), the results indicate that both the virtual velocity look angle and the predicted angular error reduce to zero upon impact. This convergence confirms that the guidance law can successfully intercept a moving target with a constant velocity, maintaining the desired impact angle without violating the missile seeker's field of view limitations.

The graph in Fig. 6(f) illustrates the missile command acceleration over time, showing that control energy increases as the desired impact angle value increases. As the missile approaches the target, the guidance command converges to zero or near zero in all cases, minimizing the control effort required at interception.

Achieving the final command acceleration at zero or near zero helps prevent command saturation near the target, thereby enhancing the overall performance of the missile. Furthermore, this results in a small attack angle at the terminal time, maximizing the warhead's effectiveness in the ATGM system.

The simulation results demonstrate the effectiveness of the proposed guidance law when applied to missiles with time-varying speed.

2) Scenario 2

In this section, we will conduct simulations in three cases with the following maximum FOV angle constraints: 1) σ_{max} = 2° 5; 2) σ_{max} = 30°; 3) σ_{max} = 45°, in both head-on and tail-chase engagement scenarios. The initial conditions and parameters of the simulation scenario in this section will continue to utilize the data provided in Table I, with the desired impact angle set to 90° for approaching targets and 70° for receding targets.

In Fig. 7, we observe the simulation results for the head-on approaching tank scenario, while Fig. 8 depicts the results for the receding tank scenario. From the simulation results in Fig. 7(a), Fig. 7(b), and Fig. 7(e), and Fig. 8(a), Fig. 8(b) and Fig. 8(e), we note that the missiles guided by the proposed guidance law all successfully intercept the target, with the terminal ZEM and impact angle errors being zero in all cases, regardless of the FOV constraints applied for both head-on and tail-chase engagements. In Fig. 7(c) and Fig. 8(c), it can be observed that the missile lead angles never exceed the prescribed FOV limits to maintain the seeker lock-on throughout the entire homing process. Particularly, no lead angle reaches its maximum value; instead, they consistently remain below the FOV limit. This establishes a robust safety margin during the homing guidance phase, reducing the risk of target lock-on loss due to external noise.

The lateral acceleration profiles for both scenarios of approaching target and receding target are displayed in Fig. 7(f) and Fig. 8(f) respectively. The simulation results depicted on the graphs show that as the look angle limit narrows, there is a greater demand for command acceleration. However, in both cases, the initial lateral acceleration values are relatively small, and gradually converge to zero or near-zero, meeting the specified requirements.

All the results of the proposed scheme have been evaluated through simulations based on the real missile environment. They have demonstrated that the proposed scheme can successfully intercept the target with the desired impact angle without violating the look-angle limits in the terminal homing guidance of air-to-surface engagement of the ATGM system. The targets in this scenario move at a constant speed. This outcome serves as evidence of the effectiveness and reliability of the proposed scheme in real combat situations.

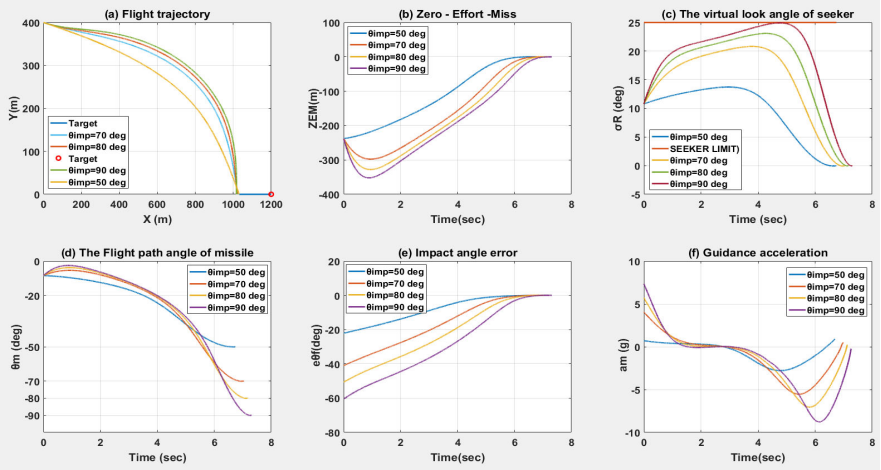

Fig. 6. Simulation results with different impact constraints in Head-on engagement.

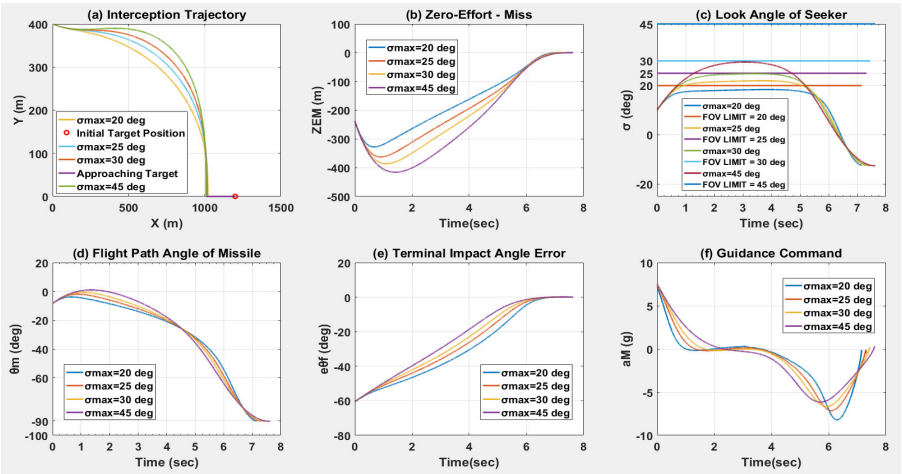

Fig. 7. Simulation results with varying FOV constrainsts in Head-on engagement.

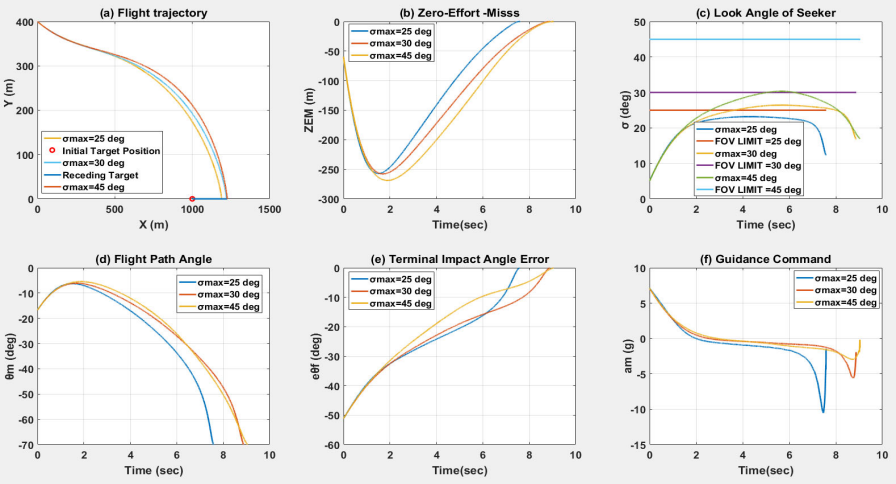

Fig. 8. Simulation results with varying FOV constraints in Tail-Chase engagement.

3) Scenario 3

In this sub-section, we will conduct simulations to evaluate the effectiveness of the synthesized guidance laws when using the weighting function *W(t)* and when not using it, as well as compare with the extended TSG guidance law [30] that has been studied in previous works:

- Case 1: Survey the extended TSG guidance law,

which has been proven to be optimal in [30] with the final approach angle constraint based on a linear system. This guidance law is based on optimal control theory, aiming to minimize the cost function of the integral of the squared command acceleration, eliminate ZEM error, and bring the final line-of-sight angle to the desired value.

The command acceleration a_{TSG} perpendicular to the missile velocity is expressed as:

$$a_{TSG} = \left(4V_C\dot{\lambda} + \frac{2V_C(\lambda - \lambda_f)}{t_{go}} \right) \Big/ \left(\cos(\theta_M - \lambda) \right) \quad (57)$$

This guidance law is denoted as "Extended TSG" on the graphs. In this context, λ_f is calculated based on the impact angle using Eq. (25), and V_C is the closing velocity.

- Case 2: The proposed guidance law without using the weighting function *W(t)* denoted as "GL without *W(t)*" on the graphs.
- Case 3: The proposed guidance law using the weighting function *W(t)* denoted as "GL with *W(t)*" on the graphs.

Our objective is to evaluate the effectiveness of the weighting function *W(t)* in shaping the trajectory and distributing the command acceleration and the look angles throughout the terminal guidance phase.

Additionally, we will compare the proposed guidance law with the existing TSG law in the scenario of a non-maneuvering moving target. The initial conditions and parameters are kept the same for all three scenarios to ensure a fair comparison, as shown in Table I. The simulation results are evaluated within the context of a head-on attack scenario.

In the case where the guidance law does not use the weighting function *W(t)*, a fixed coefficient *k* is chosen to be 5. We will also examine the terminal impact angle error and the total control expenditure of the missile required for these scenarios. The total control expenditure of the missile is defined as:

$$E = \int_0^{t_f} \left\| a_M \right\|^2 d\tau \quad (58)$$

The simulation results for all three cases are shown in the graph in Fig. 9 and Table II. Fig. 9(a)–(e) show that all guidance laws successfully intercept the target, with the final miss distance approaching zero while adhering to the desired impact angle constraints. The results in Table II show that the proposed guidance law with the weighting function *W(t)* has the most minor final impact angle error, followed by the "GL without *W(t)*" law, and the Extended TSG law having the largest terminal impact angle error. In terms of total control energy consumption, the Extended TSG law consumes the least energy, followed by the "GL with *W(t)*" law, while the "GL without *W(t)*" law consumes relatively more energy compared to the other two guidance laws.

The simulation results demonstrate that all guidance laws successfully intercept the target while complying with the constraints on the desired impact angle and FOV.

The difference between the proposed guidance laws and the Extended TSG law is clearly shown in Fig. 9(c), which depicts the look angle of the missile seeker during the terminal guidance phase. With the Extended TSG law, when not considering the field of view (FOV) limits, it violates the chosen look angle constraints during this phase, resulting in a loss of target visibility. In contrast, the proposed guidance laws successfully intercept the target with the desired impact angle without violating the ATGM system's look angle constraints.

However, with the "GL without *W(t)*" law, the look angle amplitude increases rapidly and approaches the FOV limit of the seeker. Conversely, with the guidance law using the *k(t)* coefficient varying according to the weighting function *W(t)*, the look angle amplitude increases steadily and remains within the safe FOV limit. This feature is highly desirable when designing specific guidance laws for ATGM systems using strap-down infrared imaging seekers. Rapid changes in look angle can

cause the target to move quickly across the seeker's image plane, leading to motion blur, reduced image quality, and decreased target detection performance [31].

Furthermore, the difference between the synthesized guidance laws with a variable coefficient k and a fixed coefficient k is clearly shown in the command acceleration profile in Fig. 9(f). When using a fixed coefficient k, the initial command acceleration requirement is significantly higher than with a coefficient k varying according to the weighting function $W(t)$. This leads to exceeding the missile's maneuvering limits as it enters the terminal guidance phase, causing abrupt changes at the handover point.

TABLE II. QUANTITATIVE COMPARISONS

Method	Extended TSG	GL without $W(t)$	GL with $W(t)$
Terminal impact angle error (deg)	0.0571	0.0414	0.0041
Control effort (m^2/s^3)	6,520	28,400	8,363

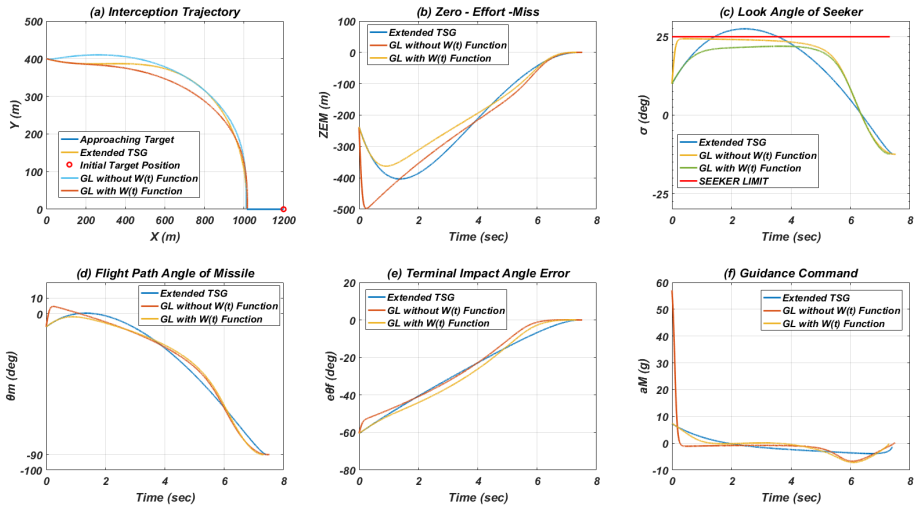

Fig. 9. Simulation results between guidance laws.

V. CONCLUSIONS

This paper presented an advanced guidance law for ATGM aimed at attacking non-maneuvering moving tanks. The proposed method integrates constraints on impact angle and addresses the FOV limitation of the missile seeker during the terminal guidance phase. Using a nonlinear virtual relative model, this method treats moving targets as stationary. The paper also introduces an optimal error dynamics form that allows the impact angle error to converge to zero within a finite time. A specially designed weighting function optimizes the distribution of command acceleration, minimizing initial guidance commands and ensuring that command magnitudes gradually reduce to zero as the missile approaches the target. A saturation function is included to effectively manage the maximum FOV angle constraint, ensuring continuous target lock capabilities of the seeker throughout the missile's flight. Numerical simulations demonstrated the robustness and high accuracy of the proposed guidance law in achieving precise impact angles while maintaining operational constraints. The results highlight the potential of the new guidance law in enhancing the tactical effectiveness of the ATGM system in real combat scenarios.

CONFLICT OF INTEREST

The authors declare no conflict of interest.

AUTHOR CONTRIBUTIONS

Dung Pham Trung and Dien Nguyen Ngoc developed the theory by contributing to the design of this research. Hai Tran Van wrote the manuscript and performed the software simulation; Tung Thanh Nguyen revised and refined the article. All authors discussed the results and commented on the manuscript. All authors had approved the final version.

REFERENCES

[1] R. Yanushevsky, *Modern Missile Guidance*, CRC Press, 2018, pp. 200.

[2] C.-K. Ryoo, H. Cho, and M.-J. Tahk, "Optimal guidance laws with terminal impact angle constraint," *Journal of Guidance, Control, and Dynamics*, vol. 28, no. 4, pp. 724–732. 2005.

[3] R. Chang-Kyung, C. Hangju, and T. Min-Jea, "Time-to-go weighted optimal guidance with impact angle constraints," *IEEE Transactions on Control Systems Technology*, vol. 14, no. 3, pp. 483–492, 2006.

[4] Park, B.-G., T.-H. Kim, and M.-J. Tahk, "Optimal impact angle control guidance law considering the seeker's field-of-view limits," in *Proc. the Institution of Mechanical Engineers, Part G: Journal of Aerospace Engineering*, vol. 227, no. 8, pp. 1347–1364, 2012.

[5] H. Cho, C. K. Ryoo, A. Tsourdos *et al.*, "Optimal impact angle control guidance law based on linearization about collision triangle," *Journal of Guidance, Control, and Dynamics*, vol. 37, no. 3, pp. 958–964, 2014.

[6] B. G. Park, T. H. Kim, and M. J. Tahk, "Range-to-go weighted optimal guidance with impact angle constraint and seeker's look angle limits," *IEEE Transactions on Aerospace and Electronic Systems*, vol. 52, no. 3, pp. 1241–1256, 2016.

[7] A. Ratnoo and D. Ghose, "Impact angle constrained interception of stationary targets," *Journal of Guidance, Control, and Dynamics*, vol. 31, no. 6, pp. 1817–1822, 2008.
[8] A. Ratnoo and D. Ghose, "Impact angle constrained guidance against nonstationary nonmaneuvering targets," *Journal of Guidance, Control, and Dynamics*, vol. 33, no. 1, pp. 269–275, 2010.
[9] K. S. Erer and O. Merttopçuoglu, "Indirect impact-angle-control against stationary targets using biased pure proportional navigation," *Journal of Guidance, Control, and Dynamics*, vol. 35, no. 2, pp. 700–704, 2012.
[10] S. R. Kumar, S. Rao, and D. Ghose, "Sliding-mode guidance and control for all-aspect interceptors with terminal angle constraints," *Journal of Guidance, Control, and Dynamics*, vol. 35, no. 4, pp. 1230–1246, 2012.
[11] X. Wang, Y. Zhang, and H. Wu, "Sliding mode control based impact angle control guidance considering the seeker's field-of-view constraint," *ISA Trans*., vol. 61, pp. 49–59, 2016.
[12] S. He, T. Song, and D. Lin, "Impact angle constrained integrated guidance and control for maneuvering target interception," *Journal of Guidance, Control, and Dynamics*, vol. 40, no. 10, pp. 2653–2661, 2017.
[13] S. He, W. Wang, and J. Wang, "Adaptive backstepping impact angle control with autopilot dynamics and acceleration saturation consideration: A robust adaptive impact angle guidance," *International Journal of Robust and Nonlinear Control*, vol. 27, 2017.
[14] H.-G. Kim, J.-Y. Lee, and H. J. Kim, "Look angle constrained impact angle control guidance law for homing missiles with bearings-only measurements," *IEEE Transactions on Aerospace and Electronic Systems*, vol. 54, no. 16, pp. 3096–3107, 2018.
[15] S. Lee, S. Ann, N. Cho *et al.*, "Capturability of guidance laws for interception of nonmaneuvering target with field-of-view limit," *Journal of Guidance, Control, and Dynamics*, vol. 42, no. 4, pp. 869–884, 2019.
[16] S. He, C. H. Lee, H. S. Shin *et al.*, Optimal guidance and its applications in missiles and UAVs. Berlin/Heidelberg, Germany: Springer, 2020, pp. 9–62.
[17] H.-G. Kim and H. J. Kim, "Field-of-view constrained guidance law for a maneuvering target with impact angle control," *IEEE Transactions on Aerospace and Electronic Systems*, vol. 56, no. 6, pp. 4974–4983, 2020.
[18] J.-Y. Lee, H.-G. Kim, and H. J. Kim, "Adjustable impact-time-control guidance law against non-maneuvering target under limited field of view," *The Institution of Mechanical Engineers, Part G: Journal of Aerospace Engineering*, vol. 236, no. 2, pp. 368–378, 2021.
[19] J. Wang, C. H. Lee, H. S. Shin *et al.*, "Field-of-view constrained three-dimensional impact angle control guidance for speed-varying missiles," *IEEE Transactions on Aerospace and Electronic Systems*, vol. 58, no. 5, pp. 3992–4003, 2022.
[20] H. T. Van, D. N. Ngoc, P. T. Dung, "Field-of-view and impact angle constrained guidance law for missile with reducing sensitivity on initial errors based on optimal error dynamics," in *Proc. 2023 12th International Conference on Control, Automation and Information Sciences (ICCAIS)*, 2023.
[21] I.-S. Jeon, H. Cho, J.-I. Lee, "Exact guidance solution for maneuvering target on relative virtual frame formulation," *Journal of Guidance, Control, and Dynamics*, vol. 38, no. 7, pp. 1330–1340, 2015.
[22] P. Zarchan, *Tactical and Strategic Missile Guidance*, American Institute of Aeronautics and Astronautics, 2012.
[23] S. Xiong, W. Wang, X. Liu *et al.*, "Guidance law against maneuvering targets with intercept angle constraint," *ISA Transactions*, vol. 53, no. 4, pp. 1332–1342, 2014.
[24] Y. Bin, W. Hui, D. Lin *et al.*, "Impact time control guidance against maneuvering targets based on a nonlinear virtual relative model," *Chinese Journal of Aeronautics*, vol. 36, no. 7, pp. 444–459, 2023.
[25] Z. Xu, H. Luo, B. Hui *et al.*, "A novel LOS rate estimation method based on images for strap-down inertial guidance," *Journal of Physics: Conference Series*, vol. 1570, no. 1, 2020.
[26] Y. Yu, K. Yi, and Q. Li *et al.*, "Guidance information estimation of the semi-strapdown infrared imaging seeker," in *Proc. 2017 36th Chinese Control Conference (CCC)*, 2017, pp. 6185–6190.
[27] M.-J. Tahk, G.-H. Moon, and S.-W. Shim, "Augmented polynomial guidance with terminal speed constraints for unpowered aerial vehicles," *International Journal of Aeronautical and Space Sciences*, vol. 20, no. 1, pp. 183–194, 2018.
[28] J. Harris and N. Slegers, "Performance of a fire-and-forget anti-tank missile with a damaged wing," *Mathematical and Computer Modelling*, vol. 50, no. 1, pp. 292–305, 2009.
[29] T-14 Armata. [Online]. Available: https://tank-afv.com/modern/Russia/T-14-armata.php#google_vignette
[30] P. Zarchan, *Tactical and Strategic Missile Guidance*, American Institute of Aeronautics and Astronautics, 2012.
[31] J.-Y. Lee and H. J. Kim, "Impact angle guidance law to prevent the detection degradation of a seeker," *The Institution of Mechanical Engineers, Part G: Journal of Aerospace Engineering*, vol. 236, no. 9, pp. 1738–1750, 2021.